Development of the GHBMC 5th Percentile Female Finite Element Model

M. L. Davis[1,2], B. Koya[1], J. D. Stitzel[1,2], and F. S. Gayzik[1,2]
[1] Wake Forest University School of Medicine, Winston Salem, NC
[2]Virginia Tech-Wake Forest University Center for Injury Biomechanics, Winston Salem, NC

ABSTRACT

To mitigate the societal impact of vehicle crash, researchers are using a variety of tools, including finite element models. Such models are often developed to represent a 50th percentile male occupant. However, in order to address the effects of size and sex-related geometrical changes, there is interest in developing such models for other cohorts. As part of the Global Human Body Models Consortium project, comprehensive medical image and anthropometrical data of the 5th percentile female (F05) were acquired. A multi-modality image dataset consisting of CT, MRI and upright MRI medical images was developed to characterize the subject in the supine, seated and standing postures. Surface topography and 52 bony landmarks were also acquired for model assembly. The selected subject closely represented the F05 in terms of height and weight, deviating less than 2% in those measures. The volunteer was also compared to 15 external anthropomorphic measurements from Gordon et al. For all 15 anthropomorphic measurements, the average subject deviation across all measures was 4.1%. The multi-modality image set was used to develop and assemble skeletal and organ components of the model. Abdominal organ volumes and cortical bone thickness were compared to literature sources where data was available. Once assembled, the segmented geometries were used for mesh development of the finite element model. Ultimately, the model consisted of 875 parts, 2.4 million elements, 1.3 million nodes, and weighed 49.3 kg. Future work will involve regional and full body level validation. Once validated, the data obtained from this model will be valuable for the development of vehicle safety devices. To date, the data set used for the development of this model is the first of its kind, acquired with the explicit purpose of developing a full-body finite element model of the F05 for the enhancement of injury prediction.

INTRODUCTION

Vehicular crash injury prevention remains a leading public health concern worldwide. In 2013, the World Health Organization reported more than 1.2 million deaths and another 20-50 million non-fatal injuries as a result of motor vehicle accidents (W.H.O, 2013). The injury outcome of vehicular crash also results in significant financial costs. In the United States alone, the National Highway Traffic Safety Administration (NHTSA) estimates the economic and

societal costs of vehicle crash at $871 billion (Blincoe, 2014). In order to design occupant protection systems that reduce risk of injury, researchers are using a variety of tools, including computational human body models (HBM). The application and development of such models is a growing component of injury biomechanics. The last 20 years has seen a large increase in the number of HBMs being developed at both the full body level (Hayes, 2014; Toyota, 2010; Yang, 2006) and body regional level (DeWit, 2012; Li, 2010; Shin, 2012; Soni, 2013). Computational HBMs, such as finite element models (FEM), are appealing because they offer a cost-effective method to evaluate and design vehicle safety devices. They are also useful for providing deeper insight into the injury mechanisms of specific tissues during dynamic loading scenarios.

Traditionally, HBMs are developed to represent an average male (50th percentile in terms of height and weight). While these models can provide a valuable assessment of the mid-sized adult male, real world motor vehicle crashes involve occupants of various size, age and gender. As an example, in the late 1990's, there was a series of fatalities resulting from airbag related injuries in otherwise low to moderate severity frontal crashes. Upon investigation, it was found that 78% of the fatalities were female, and 82% of the females were below average height (Summers, 2001). This indicated that vehicle safety features needed to be developed and tuned for drivers beyond the average sized male. From a regulatory perspective, this was addressed by including the response of a small female anthropomorphic test device (Hybrid III 5th percentile female) to evaluate the ability of vehicle safety devices to protect a wider range of occupants. In an effort to further the ability of computational models to provide comparable data, this study focuses on the model development of a female driver in the 5th percentile of height and weight (F05).

As part of the Global Human Body Models Consortium project, a comprehensive multi-modality medical image and anthropometrical dataset of the 5^{th} percentile female (F05) were acquired. This dataset is unique in that it was acquired with the specific purpose of FEM development. The objectives of this study are two-fold. The first is to present the image and anthropometrical data of the representative F05 volunteer used for the assembly of a CAD dataset of the human body. This includes both computed tomography (CT) and magnetic resonance imaging (MRI) scans obtained in the supine, seated and standing postures. Recent studies have found significant differences in abdominal organ positioning and shape between supine and seated postures (Beillas, 2009; Hayes, 2013). Therefore, in order to most accurately characterize the internal organs of a model, medical images need to be obtained in a variety of postures. The second objective is to present mesh techniques applied for development of the GHBMC F05 FEM.

METHODS

Medical Imaging Protocol and CAD Development

As an initial solicitation to identify a volunteer representing the F05, an individual with a target height and weight of 150.9 cm and 49 kg was sought. Once candidates were identified, 15 anthropomorphic measurements were acquired and compared to existing anthropometry values

presented by Gordon et al (Gordon, 1989). For inclusion in the study, the subject was to be within 5% deviation across all measurements. Applicants also had to be in generally good health and have all organs present. Additional exclusion criteria related to the imaging component of the study, such as claustrophobia and any implanted metals, were also included to ensure subject safety. The medical imaging protocol was approved by the Wake Forest University School of Medicine's Institutional Review Board (IRB, #5705).

A description of the medical imaging protocol has previously been described by Davis et al (Davis, 2014). Briefly, medical images were acquired in multiple modalities to most effectively capture varying tissue types in the seated, standing, and supine postures. The dataset was comprised of CT scans in the supine and seated posture, MRI scans in the supine posture, and upright MRI (uMRI) scans in standing and seated postures. The high resolution and relatively fast acquisition of CT scans allowed for accurate reconstruction of skeletal structures. The supine MRI images were useful for high resolution segmentation of soft tissue structures such as abdominal organs and musculature. Seated and standing uMRI scans were used to assemble geometries segmented from the higher resolution supine CT and MRI scans. The goal of this multi-modality approach was to leverage the strengths of each imaging modality in combination with posture specific acquisition to increase model biofidelity. An external anthropometry dataset was also gathered as a supplement for assembling the model in the driving posture (Davis, 2014). A 7-axis 3D FaroArm digitizer was used for collection of the subject's surface topography and external landmarks. For proper placement in the seated posture, a custom, adjustable seat buck and platform were used (Gayzik, 2012). Bony landmark data was obtained via palpation and utilized for transforming structures from the medical imaging coordinate system into the SAE J211 sign convention.

After the acquisition of the medical imaging dataset, the next major task was the development of CAD data representing the small female. The first step in this process was segmentation. Segmentation techniques consisted of a mixture of manual and semi-automatic techniques, with the tissue type dictating the approach. Standard segmentation techniques such as region growing, morphological operations, multi-slice interpolation and Boolean operations were also employed as needed. Automatic segmentation was limited to the development of gray and white matter in the brain where atlas-based algorithms were available. Bony geometries were predominately reconstructed through the use of semi-automatic methods due to the large contrast between bone and surrounding tissue. Manual segmentation was required for most other soft tissues. A more complete description of segmentation techniques can be found in the literature (Davis, 2014; Gayzik, 2011).

Segmented polygon data was then conditioned to match the position and morphology of the corresponding structures in the uMRI scans. Non-Uniform Rational B-Spine (NURBS) surfaces were developed on all assembled polygon data. Border continuity was enforced such that the patchwork was tangentially continuous (G1) with neighboring patches. With the exception of thoracoabdominal organs, the final CAD dataset was symmetric about the mid-sagittal plane.

Model Development

Mesh development for the GHBMC F05 was conducted in a fashion similar to that of the GHBMC average male model (M50) in terms of element number, size, quality, and type. In an effort to increase model robustness and stability, three of the main focuses of F05 development were 1) limiting the number of required contacts in each body region, 2) maintaining mesh uniformity throughout the model, and 3) limiting the number of intersections and penetrations between parts. To accomplish these goals, a variety of meshing techniques were employed using commercially available software. These techniques included structured hexahedral meshing, tetrahedral meshing, morphing, and element property assignment based on CAD data. Below, meshing techniques employed for each region are presented.

Head

All geometries of the cranium were developed using a structured hexahedral mesh in TrueGrid (XYZ Scientific Applications, Livermore, CA). The cranial vault and cerebrum were developed as a continuous mesh to ensure the quality of the brain-to-skull interface. The posterior surface of the brainstem is connected node-to-node with the cerebellum and the superior surface is connected to the cerebrum via the mid-brain. Remaining geometric features within the brain were developed using element assignment techniques based off of the CAD data. These techniques were used to maintain the node-to-node connection throughout the brain. The solid geometries of the face, with the exception of the mandible, were hexahedrally meshed in TrueGrid. Because of the similarity in shape between the F05 and M50 mandible, this geometry was morphed from the M50 using ANSA software (BETA CAE, Thessaloniki, Greece). Examples of the head mesh of the F05 can be seen in Figure 1.

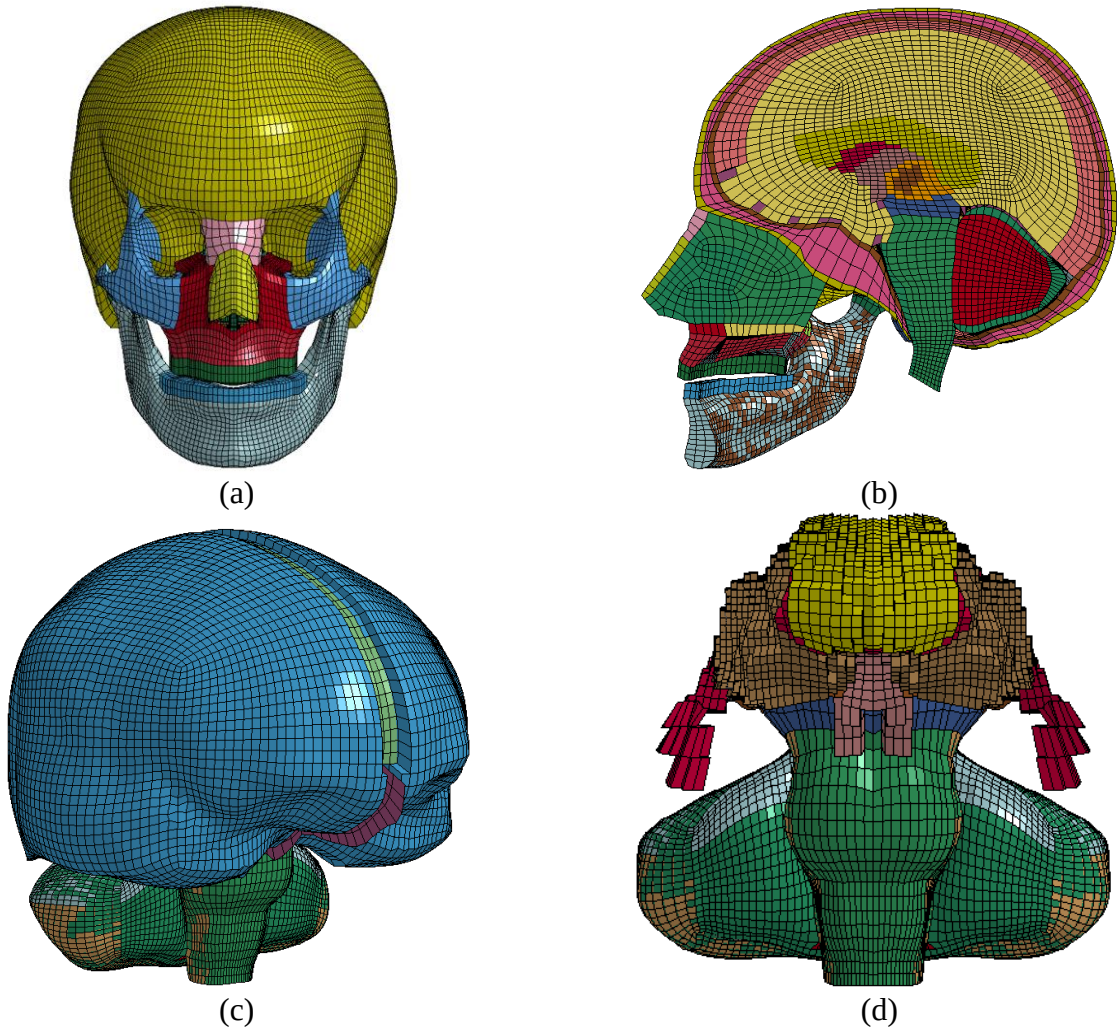

Figure 1: Skull and brain of the F05.

Neck

The neck region of the model was predominately meshed using hexahedral elements. The exceptions were tetrahedral transition regions used to develop node-to-node connections at the origin and insertion sites of the 52 explicitly represented neck muscles. The solid hexahedral elements of the cervical spine were used to represent trabecular bone, with quadrilateral shell elements used to characterize cortical bone. The facets of each cervical vertebrae were developed via extrusion from the surface of transverse process. The intervertebral discs (IVDs) at each vertebral level of the model were separated into two parts representing the nucleus and ground substance of the disc. In addition, the ground substance of each IVD was modeled with four layers of elements in the anterior-posterior direction to allow the inclusion of five annulus fibrosis layers as shell elements. Images of the F05 neck region can be seen in Figure 2.

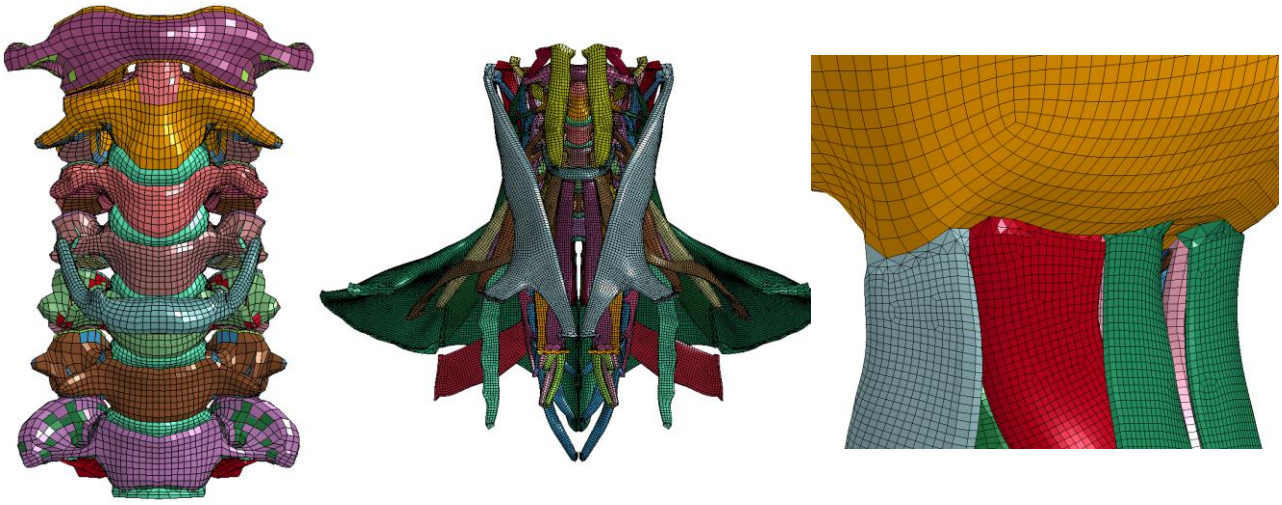

Figure 2: F05 neck mesh. Left) Cervical Spine with intervertebral discs. Middle) 52 explicitly represented neck muscles. Right) Example of node-to-node attachment of neck muscle at insertion.

Thorax and Upper Extremity

The sternum, ribs, and costal cartilage were developed using a structured butterfly mesh topology in TrueGrid. Two shell layers were implemented between each rib to represent the internal and external intercostal muscles. The heart, lungs, aorta, vena cava, and secondary large vessels were also hexahedrally meshed. Long bones of the upper extremity (humerus, radius, and ulna) were morphed from the M50 using the approach discussed above. Because they are modeled as rigid parts, the thoracic vertebrae were also morphed from the M50 to the CAD of the F05. Similar to the cervical spine, cortical bone in the thoracic region was applied as shell elements. Major joints of the torso region, such as the costovertebral, acromioclavicular, and sternoclavicular joints, were modeled with 0-length, 6 degree-of-freedom beams with prescribed stiffness about each axis of rotation.

The flesh and muscle of the thorax were modeled as a continuous mesh with muscle CAD being used to assign element material properties rather than explicitly meshing CAD geometry. Using this approach, the flesh of the upper extremities was meshed continuously from the outer surface down to the bone. At the joints of the arm, the flesh was meshed using tetrahedral elements. At the shoulder and elbow joints where the muscles connect, CAD data was used to explicitly mesh muscle connections to the bone. With regards to the main thoracic flesh, the pectoralis major, latissimus dorsi, and rhomboid major were developed via element assignment. Images of the F05 thorax and techniques employed for musculature can be seen in Figure 3.

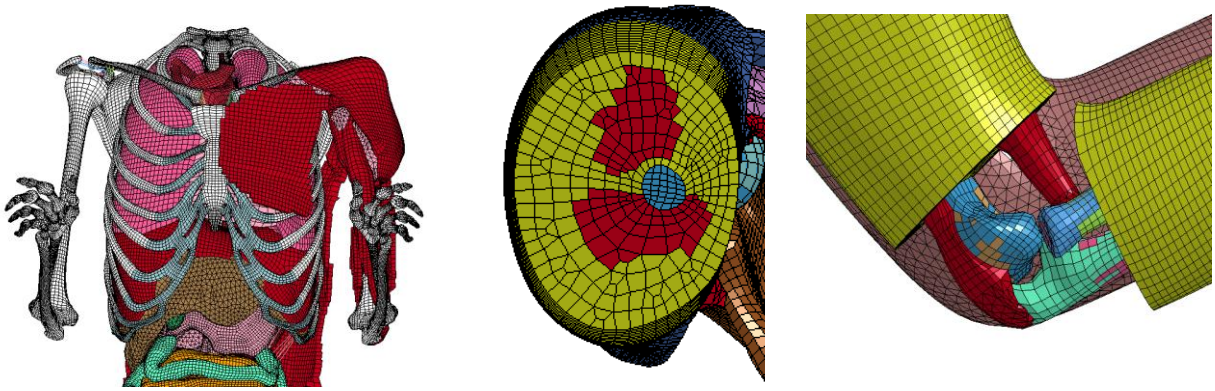

Figure 3: Left) Internal thoracic components of the F05 model. The anterior muscles on the right side have been removed for visualization. Middle) Cross-section of humerus showing continuous mesh with bone, muscle, and flesh. Right) Explicitly modeled musculature at insertion site.

Abdomen and Pelvis

Similar to the M50, the abdominopelvic region of the F05 is tetrahedrally dominant. The liver, spleen, kidneys, gallbladder, and pancreas were modeled with solid elements and a layer of shell elements on the outer surface representing parenchyma. Due to severe compression of the abdomen in blunt impact scenarios, the remaining abdominal structures were modeled as airbags to increase model robustness. Also, the small intestine was modeled as a control volume due to its geometric complexity. During CAD development, an abdominal compartment was created from the seated uMRI data by surrounding all of the organs and abdominal fat deep to abdominal muscles. This compartment was utilized for the development of abdominal fat by employing Boolean relationships to characterize space within the compartment not occupied by organs.

The flesh and muscle of the abdominal region were modeled as a continuous mesh with muscle CAD being used to assign element material properties. Because the more superficial abdominal muscles serve mainly for passive load transfer, specific muscles were grouped to simplify the region. For example, the rectus abdominis and obliques were combined into one part with the same material type. The psoas major is the one exception for muscle development in the abdomen. The psoas was explicitly meshed using tetrahedral elements and connected node-to-node with the lumbar spine and the pelvis. Detailed images of the abdominopelvic region can be seen in Figure 4.

Figure 4: Left) F05 abdominal organs. Middle) Sagittal cross-section showing continuous flesh mesh and abdominopelvic cavity. Right) Bones and muscle of the pelvic region.

Lower Extremity

The lower extremity of the F05 model was primarily meshed using hexahedral elements. The diaphyses of the femur and tibia were modeled with solid cortical bone elements and a void representing the medullary canals. Due to restrictions based on minimum element size, the fibula was modeled with solid trabecular elements throughout the structure with shells representing cortical bone. The cruciate and collateral ligaments (ACL, PCL, MCL, LCL) were each modeled using 3D hex elements and connections to bones were made node-to-node. Cartilage of the knee was modeled from the corresponding bone surfaces using shell elements. The menisci were hex-mesh from the CAD and connected node-to-node to the tibia

The flesh and muscle of the lower extremity were continuously meshed to limit the number of required contacts. In the upper leg, muscles were grouped to have parts representing the quadriceps and the hamstrings. The muscles of the lower leg consisted of the grouped calf muscles (soleus and gastrocnemius) and the tibialis anterior (Figure 5). The approach to these muscles was similar to that of the upper extremity, where the main body of the muscle was developed by element assignment and the origin/insertion connections were developed explicitly from the CAD.

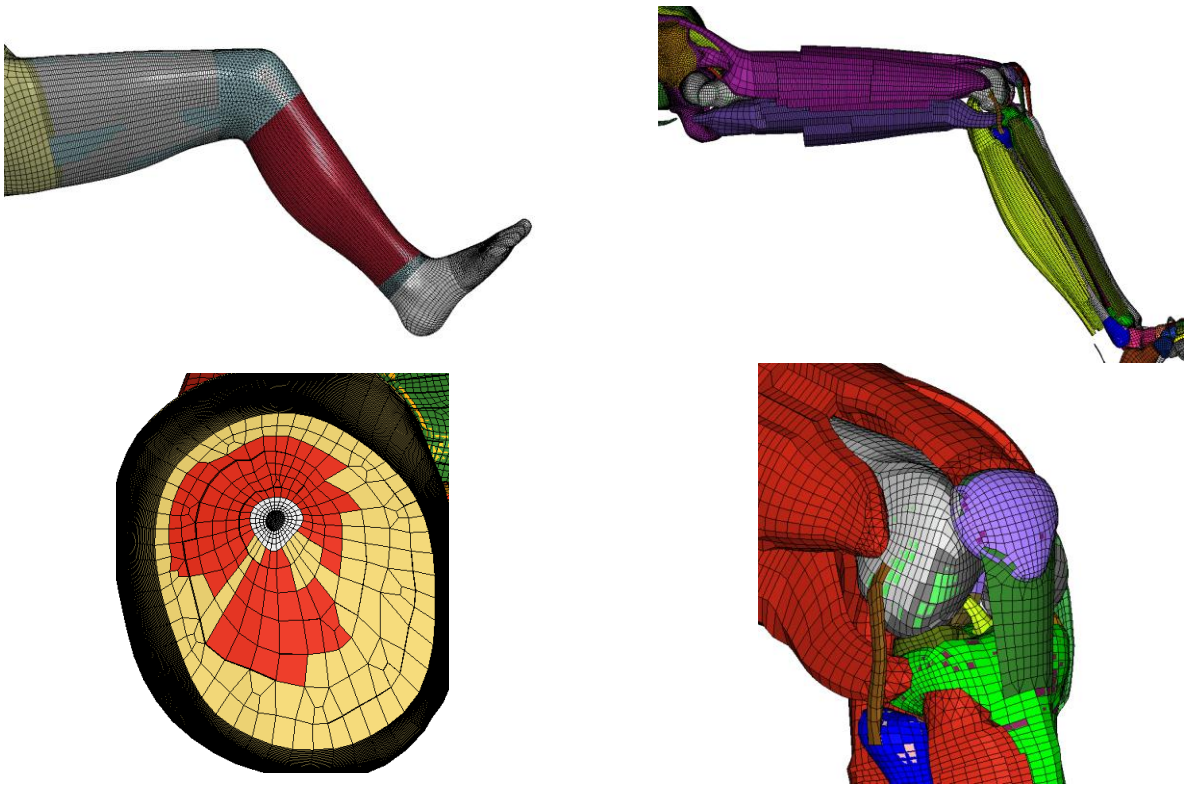

Figure 5: Flesh and muscle of the lower extremity.

RESULTS

Medical Imaging and CAD Development

The selected volunteer was a good fit in terms of height and weight (149.9 cm, 48.1 kg) with deviations from the target values of 0.7% and 1.9% respectively. For all 15 external anthropomorphic measurements taken from Geraghty et al., the average subject percent deviation was 4.1% (threshold for inclusion was 5%) (Gordon, 1989). Data on each measurement has previously been reported in the literature (Davis, 2014).

In total, 66 scan series were collected across all modalities for a total of 14,170 images. Using this data, 3D CAD geometries were developed for all skeletal structures and each organ that was explicitly modeled. The skeleton consists of 182 individual bones. Explicit representations of 32 organs were developed, encompassing brain, thoracic, and abdominal organs relevant to biomechanical modeling. An in-depth review of structures included in the F05 CAD dataset can be found in the literature (Davis, 2014). Figure 6 displays the assembled CAD model of the F05.

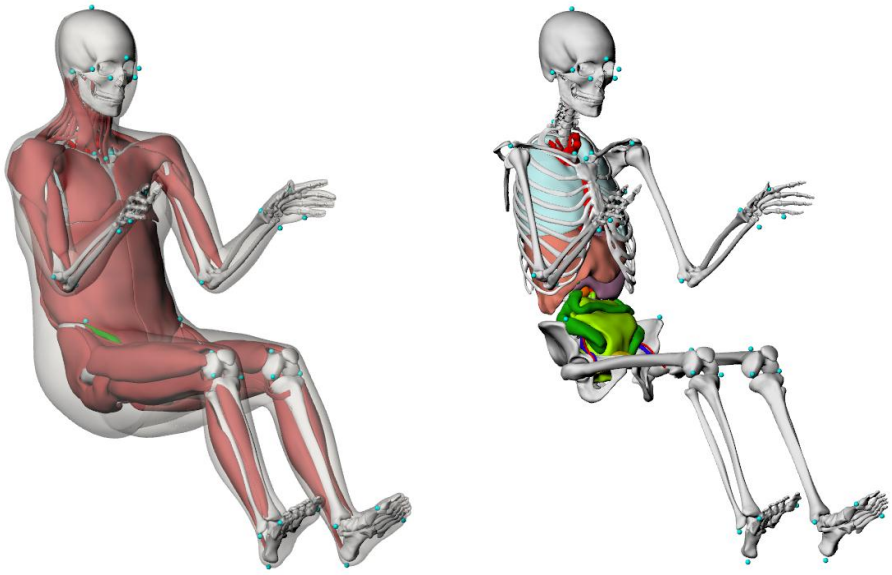

Figure 6: F05 occupant CAD model.

Finite Element Model Development

The alpha version of the GHBMC F05 occupant model has been completed and is currently undergoing validation at both the regional and full-body levels. Regional validations are being conducted by partner research institutions. Summary statistics of the F05 model can be found in Table 1. The model was developed with a target element edge length of 2-3 mm. With regards to element quality, stringent thresholds were placed on several criteria: Jacobian (>0.3 for all solid elements and >0.4 for all shells), tet-collapse (>0.2 for all elements), zero intersections, and a minimum time step value of 0.1 μs. The goal for these hard targets was to have 100% adherence to the standards. Additional element quality criteria were also in place with a target of 99% compliance for all elements. A review of the number of elements by element type and by body region can be found in Figure 7 and Figure 8 respectively.

Table 1: F05 Occupant Summary Statistics.

	F05 α	M50 v4.3
Number of Parts	875	997
Number of Elements	2.4×10^6	2.2×10^6
Number of Nodes	1.3×10^6	1.3×10^6
Model Mass (kg)	49.3	77.0
Number of Contacts	21	449

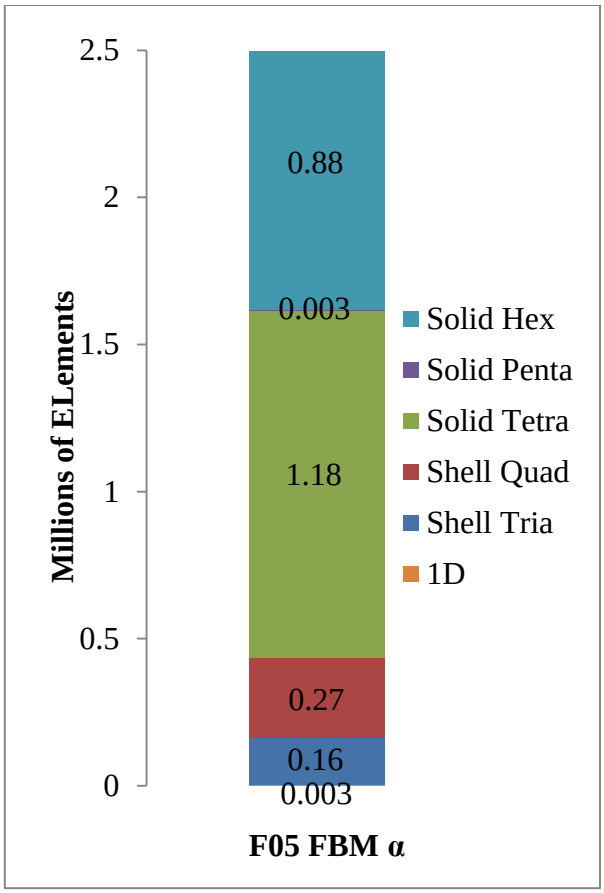

Figure 7: Element breakdown by element type within the full body model.

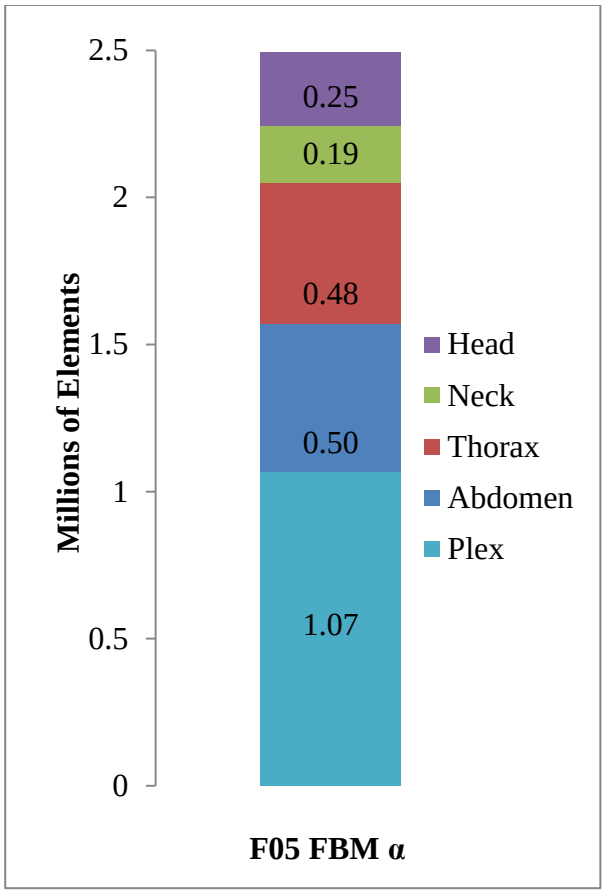

Figure 8: Element breakdown by body regional model.

In total, 691 unique material definitions were used to characterize parts within the model. To expedite development, material models were primarily carried over from the average male model (GHBMC M50-O v. 4.3). This approach not only provides a baseline for model development, but also facilitates comparisons to the GHBMC M50.

The use of node-to-node connections and element assignment techniques, where appropriate, significantly reduced the number of required contacts as compared to the GHBMC M50 model. For example, the femur, quadriceps, hamstrings, and thigh flesh were all developed using a continuous mesh, removing the need for a contact between these parts. The alpha version of the model currently implements 21 contacts, which is a 95.3% reduction in the number of contacts compared to the M50. The goal of this reduction was to reduce the computational demand of the model while increasing model robustness. The assembled F05 occupant model can be seen in Figure 9.

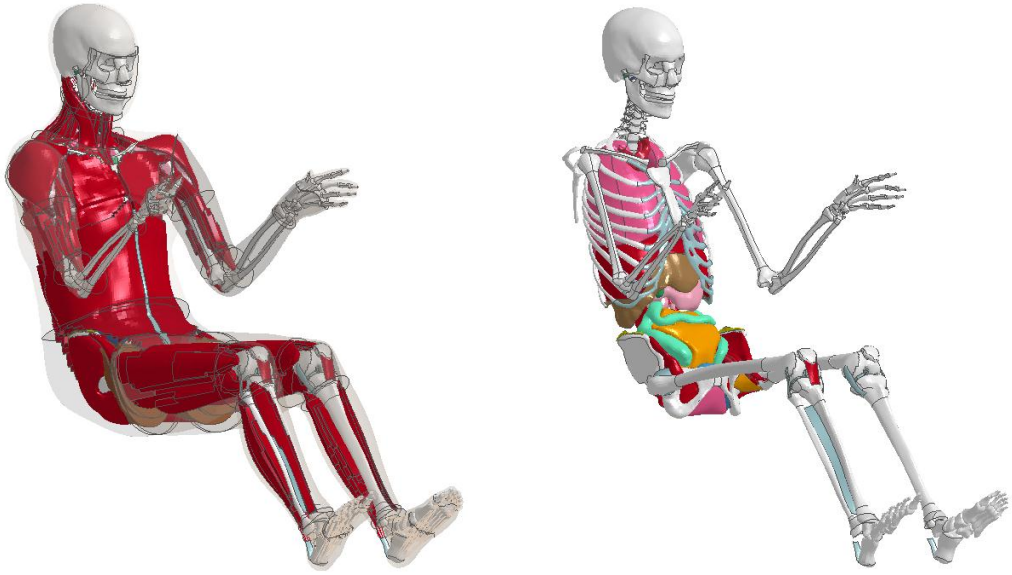

Figure 9: F05 occupant finite element model.

DISCUSSION

This study presents the development of a detailed human body finite element model of a representative 5th percentile female. The model is unique in that its geometry and assembly were based on an extensive external anthropometry and multi-modality image dataset of a specific subject matching small female anthropometry, specifically collected for the purpose of FEA model development. This approach provided detailed data of both bony tissue and internal structures and their relative orientation in a driving posture. The full dataset was leveraged, where appropriate, to facilitate model reconstruction. Assembly of skeletal structures in the model coordinate system was completed using the external anthropometry dataset and bony structures placed in the seated CT scans. Seated uMRI scans were used for assembly of abdominal organs to ensure correct shape and position.

The height and weight requirements for the F05 were based on nominal values used for development of the HIII F05 anthropomorphic test device (ATD). This approach was taken because the HIII F05 will ultimately be used as an important point of comparison for the F05 FEM. This allows for direct comparison to a model that is already an integral part of the regulation processes for the evaluation of vehicle safety performance. To further compare the models, the assembled skeleton of the GHBMC F05 was compared to the HIII F05 based on a number of external anthropometry measurements, such as arm length, shoulder breadth, etc. For the observed anthropometry, the F05 was found to closely match the HIII F05, with an average deviation of 2.7% (Davis, 2014).

The anatomical components identified for inclusion within the model were selected specifically for the evaluation of crash induced injury. However, other structures designed to

facilitate passive load transfer and promote accurate kinematics were also included. For example, secondary branches of the aorta, vena cava, and hepatic portal vein were included due to their natural role as a tether for abdominal organs. Because this model will ultimately be used for the evaluation of tissue response to blunt impact, much of the microvasculature of the human body was not included. This approach was taken since final model validation will be compared to empirical data obtained from experiments conducted at the organ or full-body levels.

One of the main limitations of this work was the sample size used for model development. However, this was a pragmatic decision made to enhance the practicality of the study. The careful recruitment of one anthropometrically representative female allowed for the collection of an extensive external anthropometry and medical imaging dataset that would not have been feasible with additional volunteers. By taking this approach, medical imaging data was available to validate results of the developed geometries. Another limitation was the limited data in the literature specific to the F05. Where possible, medical images of representative small females were consulted for additional validation. This approach was used for verification of thoracoabdominal organ volumes (Davis, 2014). This study established an estimated target for individual organ volumes of a representative 5^{th} percentile female based on stature and body mass index. Based on the results from this study, the thoracoabdominal organs of the F05 model were found to be within normal ranges of small females. In particular, the F05 was found to be within the representative error for all estimates of 5^{th} percentile female organ volumes.

Future work will be centered on model validation at both the regional and full body levels. Validation of the main body regions discussed in the methods will be conducted by partnering academic research centers (see Acknowledgements). The continued development of the model will be conducted in an iterative fashion; modifications introduced in regional testing will integrated into the full body model for full body validation. Full body validation simulations will be run in a number of different loading scenarios, such as rigid hub impacts and sled tests. Future work will also explore various methods of scaling and how they can be applied to the small female to facilitate comparisons to models with varying anthropometries.

CONCLUSIONS

An alpha version of the GHBMC F05 FEM has been developed. The model is unique in that it was developed from an extensive dataset based on a single, living subject representing a small female. The model includes detailed bony and soft tissues relevant to assessing crash induced injuries. Throughout development, both internal and external geometries were compared to published literature and regulation standards for anatomical validation. The F05 model has 2.4 million elements, 1.3 million nodes, and weighs 49 kg. Through the use of node-to-node connections and element assignment techniques, development of the F05 sought to substantially limit the number of required contacts to enhance computational efficiency. At its current state of development the F05 model employs 95.3% fewer contacts than the GHBMC M50 model. Future work with the model will focus on regional and full body validation, with a focus on methods to apply scaling techniques for model validation.

ACKNOWLEDGEMENTS

Funding for this study was provided by the Global Human Body Models Consortium, LLC through GHBMC Project Number: WFU-005. The authors gratefully acknowledge the contributions of the Body Region Centers of Excellence (COE) in the GHBMC for advice during model development and ongoing regional validation of the model. The GHBMC BRM COEs are located at Wayne State University (Head COE, PI Liying Zhang), The University of Waterloo (Neck COE, PI Duane Cronin), The University of Virginia (Thorax, Pelvis, and Lower Extremity COE, co-PIs Matt Panzer, Rich Kent, and Jeff Crandall), and IFSTARR (Abdomen COE, PI Phillipe Beillas).

REFERENCES

Beillas, P., Lafon, Y., Smith, F. W. (2009) The effects of posture and subject-to-subject variations on the position, shape and volume of abdominal and thoracic organs. Stapp Car Crash J 53: 127-54.

Blincoe, L., Miller, T.R., Zaloshnja, E., and Lawrence, B.A. (2014) The Economic and Societal Impact of Motor Vehicle Crashes, 2010.

Davis, M.L., Allen, B.C., Geer, C.P., Stitzel, J.D., and Gayzik, F.S. (Year) A Multi-Modality Image Set for the Development of a 5th Percentile Female Finite Element Model. Proc. International Research Council on Biomechanics of Injury.

Davis, M.L., Stitzel, J.D., and Gayzik, F.S. (2014) Thoracoabdominal organ volumes for small women. Traffic injury prevention (just-accepted): 00-00.

DeWit, J.A., and Cronin, D.S. (2012) Cervical Spine Segment Finite Element Model for Traumatic Injury Prediction. Journal of the Mechanical Behavior of Biomedical Materials 10: 138-150.

Gayzik, F.S., Moreno, D.M., Geer, C.P., Wuertzer, S.D., Martin, R.S., and Stitzel, J.D. (2011) Development of a Full Body CAD Dataset for Computational Modeling: A Multi-Modality Approach. Annals of Biomedical Engineering 39 (10): 2568-2583.

Gayzik, F.S., Moreno, D.P., Danelson, K.A., McNally, C., Klinich, K.D., and Stitzel, J.D. (2012) External Landmark, Body Surface, and Volume Data of a Mid-Sized Male in Seated and Standing Postures. Annals of Biomedical Engineering 40 (9): 2019-32.

Gordon, C.C., Churchill, T., Clauser, C.E., Bradtmiller, B., and McConville, J.T. (1989) Anthropometric survey of US army personnel: methods and summary statistics 1988. DTIC Document.

Hayes, A.R., Gayzik, F.S., Moreno, D.P., Martin, R.S., and Stitzel, J.D. (2013) Abdominal Organ Location, Morphology, and Rib Coverage for the 5(th), 50(th), and 95(th) Percentile Males and Females in the Supine and Seated Posture using Multi-Modality Imaging. Ann Adv Automot Med 57: 111-22.

Hayes, A.R., Vavalle, N.A., Moreno, D.P., Stitzel, J.D., and Gayzik, F.S. (2014) Validation of simulated chestband data in frontal and lateral loading using a human body finite element model. Traffic Inj Prev 15 (2): 181-6.

Li, Z., Kindig, M.W., Kerrigan, J.R., Untaroiu, C.D., Subit, D., Crandall, J.R., and Kent, R.W. (2010) Rib Fractures Under Anterior-Posterior Dynamic Loads: Experimental and Finite-Element Study. Journal of Biomechanics 43: 228.234.

Shin, J., Yue, N., and Untaroiu, C.D. (2012) A finite element model of the foot and ankle for automotive impact applications. Ann Biomed Eng 40 (12): 2519-31.

Soni, A., and Beillas, P. (2013) Modelling hollow organs for impact conditions: a simplified case study. Comput Methods Biomech Biomed Engin.

Summers, L., Hollowell, W.T., and Prasad, A. (Year) Analysis of occupant protection provided to 50th percentile male dummies sitting mid-track and 5th percentile female dummies sitting full-forward in crash tests of paired vehicles with redesigned air bag systems. Proc. Proceedings of the 17th International Technical Conference on the Enhanced Safety of Vehicles, Amsterdam, The Netherlands.

Toyota (2010) Documentation of Total Human Model for Safety (THUMS) AM50 Pedestrian/Occupant Model. Toyota Motor Corporation.

W.H.O (2013) Global status report on road safety. ed. W. H. Organization. World Health Organization, Geneva, Switzerland.

Yang, K.H., Hu, J., White, N.A., King, A.I., Chou, C.C., and Prasad, P. (2006) Development of Numerical Models for Injury Biomechanics Research: A Review of 50 Years of Publications in the Stapp Car Crash Conference. Stapp Car Crash J 50: 429-90.